

Synthesis of Core-Shell Particles of Polystyrene and Poly(methyl methacrylate) Using Emulsion Photopolymerization

D. L. Chicoma, V. Carranza, R. Giudici*

Summary: Submicron core-shell particles of polystyrene (PS) and polystyrene-co-poly(methyl methacrylate) (PS-co-PMMA) coated with PMMA were obtained by emulsion photopolymerization. The seeds of PS or PS-co-PMMA were prepared by emulsion polymerization with or without emulsifier and a ratio of functional monomer and crosslinker (SVBS/EDGMA) in order to obtain different surfaces for the subsequent coating with PMMA. At each stage, the evolution of the average particle size were monitored by using photon correlation spectroscopy (DLS) and the final polymer particles was analyzed via transmission electron microscopy (TEM) and differential scanning calorimetry (DSC). The core-shell morphology was identified as the increase of the average particle size in the second stage by DLS technique and by the direct observation by TEM of the differentiation between PS core and PMMA shell, and by the presence of two glass transition temperatures (T_g) as a consequence of the existence of two partially miscible phases.

Keywords: core-shell particles; emulsion photopolymerization

Introduction

In recent decades, considerable efforts have been devoted to the preparation and control of nanostructured materials, because the physico-chemical properties of these materials changes as a function of the size, composition and structure of the particles. The development of suitable methods for control the synthesis of these materials has been object of efforts of different laboratories and industrial research in fields such as engineering, pharmacy and biomedical research.

In recent years, nanoparticles with 'core-shell' structure has been satisfactorily applied in coatings, electronics, catalysts, separation and diagnosis materials because they present special and interesting optical and surface properties in comparison with

simple particles.^[1] However, the preparation of core-shell particles requires special care, particularly in the formation and stability of the shell and the prevention of the aggregation of the particles. Thus, various polymerization strategies have been used to produce polymer particles coated with a shell of a different polymeric material, such as the modification of the surface of the core particles to facilitate the adhesion of the shell with one or several layers^[2] and also adsorption of the monomer in the particle.^[3–5]

Photopolymerization/photocuring processes has grown in recent decades due not only to the large number of new applications but also its impact in economic, technical and ecological terms^[6] and is important in areas such as dentistry,^[7] optics,^[8] graphical arts and printing inks^[9,10] as well as in electronics.^[11] The technique consists of incidence of light radiation in the ultraviolet-visible (UV/vis) region on the monomer with a photoinitiator for radical generation responsible for obtaining

Universidade de São Paulo, Escola Politécnica - Department of Chemical Engineering, Av. Prof. Luciano Gualberto, travessa 3, No. 380, 05508-010, São Paulo, SP, Brasil
E-mail: rgjudici@usp.br

a polymer dispersed in an aqueous medium. This technique presents several advantages over other polymerization processes, e.g., the formulation can be solvent-free (which reduces levels of VOC) and the high reaction rates can be obtained at low temperatures for production of polymers with high molecular weights. This technique has been used for the preparation of nanostructured particles with modified, functionalized surfaces, preparation of blends of two structures as a bi-continuous phases,^[12] or LC polymer network structures^[13] and polymer emulsions as presented by Shim et al.,^[14] where prepared particles of PMMA synthesized an iniferter photoinitiator (initiator and transfer agent radicals) in a RAFT polymerization process at temperatures between 60 and 80 °C in the absence of surfactant and conventional initiator. Silveiras et al.^[15] studied the production of a prepolymer with a narrow molecular weight distribution from a reaction of free radical polymerization of MMA in batch regime with photoinitiator benzoin and found that the initial concentration of the photoinitiator and the time exposition to the UV radiation are key parameters in the production of the prepolymer consisted of a mixture of 5–20% of PMMA in MMA.

Relatively few papers were found in the scientific literature on the use of this photopolymerization technique for producing micro-encapsulated material or core-shell particles. Guo et al.^[16] synthesized a layer of poly(acrylic acid) in the form of “sticks” (brushes) on the surface of polystyrene particles by the technique of emulsion photopolymerization. For this purpose, the surfaces of polystyrene particles, prepared from a conventional emulsion polymerization, were coated with the slow addition of a photoinitiator (2-[*p*-(2-hydroxy-2-methylpropiophenone)]-ethylene glycol-methacrylate 2 (HMEM) then, after washing the latex, the acrylic acid was added. The photopolymerization was conducted by using the UV/vis radiation at a temperature of 25 °C. The authors reported that the synthesis of poly(acrylic acid) is

affixed on the surface of the polystyrene particles with a well-defined morphology and a narrow distribution. In another work, Lu et al.^[17] successfully synthesized nanoparticles formed with a PS core covered with a cross-linked poly(*N*-isopropylacrylamide) shell (PNIPA) using the technique of photoemulsion polymerization. The results indicated that monodisperse PS-NIPA core-shell particles with different cross-linking densities have been successfully synthesized by this technique, presenting a homogeneous regular PNIPA shell on the spherical PS core. Schrinner et al.^[18] produced PS particles with electrosteric stabilization by the incorporation of a thin layer of photoinitiator HMEN (compound synthesized by initiator Irgacure 2959 and methacrylic acid hydrochloride) and acrylic acid monomer on the particle surface. The obtation of this particle morphology of surface modified (PS-co-HMEN-PAA) was performed in a novel UV reactor seeking a new large-scale production. Finally, Balta et al.^[19] studied the production of PMMA by photoinitiated free radical polymerization in aqueous solution using chemical incorporation via hydrogen abstraction mechanism of the tioxanthone into β -cyclodextrin as photoinitiator (type II), indicating the advantage of its efficiency over benzophenones type photoinitiators.

In the present work, seed particles were prepared from the emulsion polymerization of polystyrene (PS) and copolymer polystyrene-co-polymethyl methacrylate (PS-co-PMMA) under different operational conditions. The seeds were then coated with PMMA using the technique of emulsion photopolymerization, using benzoin as photoinitiator. During each stage, the particle growth was monitored by measuring the average particle size by dynamic light scattering/photon correlation spectroscopy (DLS). The formation of the final morphology of nanostructured particles was investigated using transmission electron microscopy (TEM) and thermal analysis using differential scanning calorimetry (DSC).

Experimental Part

Materials

Monomers styrene (S) and methyl methacrylate (MMA) kindly provided by BASF, Brazil; sodium 4-vinylbenzene sulfonate (SVBS) as functional co-monomer, water-soluble initiator potassium persulphate (KPS), benzoin as photoinitiator, ethylene glycol dimethacrylate (EGDMA) as cross-linking agent, sodium lauryl sulfate (SLS) as emulsifier, sodium bicarbonate (NaHCO_3) as buffer agent and deionized water were used in the experiments. Reactor content was flushed with a nitrogen stream by avoid inhibition of the polymerization process and a hydroquinone solution (1%) was used to shortstop the reaction in the samples taken from the tank reactor or the photochemical reactor.

Measurements

Samples periodically taken from the reactor during the polymerizations were analyzed for residual monomers via gas chromatography (GC-17A, Shimadzu) and average particle size (D_p) by dynamic light scattering (DLS) with a Coulter N4 Plus equipment using the angle of incidence of photons at 90° .

The morphology of the polymer particles was investigated by transmission electron microscopy (TEM) (LEO 906E model). The latex samples were dried in an oven for 24 h at a constant temperature of 60°C . After drying, a sufficient amount of this material was placed on the base

of the mold with epoxy resin (Polybed-Araldite, Polisciences), then the mixture was centrifuged at 10,000 rpm for ten minutes, thereby creating a homogeneous dispersion of the sample in the resin matrix. This mixture was cured in an oven at 60°C for 48 h and then cut in ultrathin slices of thickness between 60 and 100 nm using a diamond knife (Diatome, 458) and an ultramicrotome (Ultracut R, Leica) at room temperature. The slices were placed onto TEM copper grids (200 mesh) and staining with RuO_4 vapor for 8 h. After chemical staining, the slices were coated with a thin layer of carbon to prevent degradation of the PMMA sharp front exposure to the electron beam, and then followed to the TEM operated with power 80 kV.

Thermal analysis of the samples were performed with a differential scanning calorimeter (DSC) Shimadzu model DSC-60 coupled to an FC-60-A, under a nitrogen atmosphere (100 mL/min) using a heating rate of $5^\circ\text{C}/\text{min}$ from 25 to 150°C .

Synthesis of Core Particles by Emulsion

Polymerization

Seeds of PS and PS-co-PMMA with different sizes and surface characteristics were prepared by emulsion polymerization with the recipes presented in Table 1. The reactions include nucleation micellar conventional (micellar nucleation, runs CS73 and CS74), emulsifier-free (homogeneous nucleation, runs CS77 and CS81) emulsion polymerization and use of SVBS/EDGMA (runs CS78 and CS79) in the absence of

Table 1.

Recipes used in the production of seeds (core particles) of PS e PS-co-PMMA.

Reactants*	CS77** (PS)	CS81** (PS-PMMA)	CS78*** (PS)	CS79*** (PS-PMMA)	CS73**** (PS)	CS74**** (PS-PMMA)
S	0.1	0.05	0.1	0.05	0.1	0.05
MMA	–	0.05	–	0.05	–	0.05
$\text{K}_2\text{S}_2\text{O}_8$	$9.4\text{E-}4$	$9.4\text{E-}4$	$1.5\text{E-}3$	$1.5\text{E-}3$	$1.5\text{E-}3$	$1.5\text{E-}3$
SLS	–	–	–	–	$1.04\text{E-}3$	$1.04\text{E-}3$
NaHCO_3	–	–	–	–	$5.0\text{E-}4$	$5.0\text{E-}4$
SVBS	–	–	$1.0\text{E-}4$	$1.0\text{E-}4$	–	–
EGDMA	–	–	$2.0\text{E-}3$	$2.0\text{E-}3$	–	–
Water	0.8975	0.8975	0.8964	0.8964	0.897	0.8975
Final Conversion	0.97	0.99	0.99	0.99	1.0	1.0

*Mass fraction. ** free-emulsifier, *** SVBS/EDGMA ratio, **** with SLS.

emulsifier. All reactions were carried out in a jacketed glass reactor (Figure 1a) under batch regime at a temperature of 80 °C and an agitation of 350 rpm. For the emulsifier-free polymerization reactions, the most suitable ratio of SVBS/EDGMA was found to be 0.055, while a greater amount of crosslinker in relation to SVBS may cause destabilization/particle coalescence in the reaction medium. It is noteworthy that this ratio reduced the reaction time compared to the work reported in the literature^[20–23] for free-emulsifier reactions, achieving high conversions in approximately 6 hours.

Synthesis of Shell by Emulsion Photopolymerization

For the formation of core-shell particles, polymerization of MMA over the seed particles was performed using a glass photoreactor (UV-Consulting Peschl) with a Duran medium-pressure mercury lamp (Model N-HPL 125 W) inserted into a cooling jacket well (Figure 1b). The recipe of these runs is presented in Table 2. The reactions for seed coating were carried out in starved semibatch mode, with a slow feed of monomer MMA mixed with benzoin photoinitiator. The total reaction time was

Table 2.

Recipe of the shell formation reactions (emulsion photopolymerization)

Reactants	Mass fraction
Water	0.6967
Benzoin	0.0012
MMA	0.0580
Seed polymer	0.2442

180 minutes. The temperature of the reactor content was controlled within the range 32 ± 2 °C by the flow of the cooling water circulating in the well of the UV lamp and a thermostatic bath maintained at 15 ± 1 °C. The homogenization of the reactor content was performed using a magnetic stirrer. Inert gas nitrogen was bubbled in the reactor to prevent inhibition by oxygen and also help to promote mixing of the reaction medium.

Results

Table 3 presents the results of the final conversion obtained in the second stage (photopolymerization) as well as the average particle size after each polymerization stage. Figure 2 presents the evolution of the

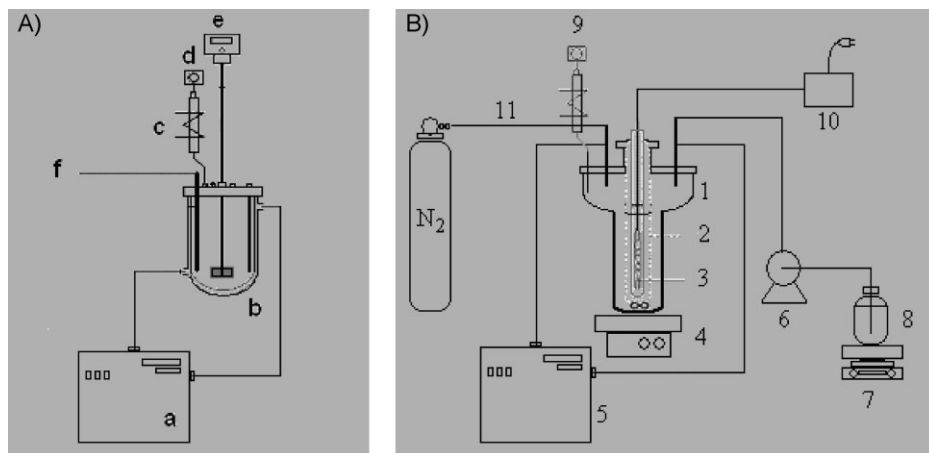


Figure 1.

A) Schematic of the experimental setup: a–thermostatic bath, b–jacket glass tank reactor, c–cooling water, d–condenser, e–stirrer, f–nitrogen stream for blanketing. **B)** Schematic of the photoreactor unit. 1–photoreactor, 2–lamp well cooling jacket, 3–UV lamp, 4–magnetic stirrer, 5–thermostatic bath, 6–dosing pump, 7–balance, 8–feeding tank of monomer or initiator, 9–condenser, 10–power source for the UV lamp, 11–feeding of nitrogen for blanketing.

Table 3.Results of global conversion (X) and average particle size (D_p) for emulsion photopolymerization reactions.

	FP25**	FP26**	FP28***	FP27***	FP23****	FP24****
Final Conversion (X)	0.93	0.92	0.92	0.95	0.92	0.91
Particle Size (nm)						
Core	460.8 (CS77)	393.8 (CS81)	308.7 (CS78)	311.3 (CS79)	98.5 (CS73)	92.1 (CS74)
SD* core	148.3	126.4	132.3	72.3	21.4	22.6
Shell	676.6	368	437.9	514.9	154.5	130.4
SD* shell	236.5	105.9	132.3	162.4	21.4	32.9

*Standard deviation ** free-emulsifier, *** SVBS/EDGMA ratio, **** with SLS.FP25, FP28 and FP23 = PS/PMMA system. FP26, FP27 and FP24 = PS-co-PMMA/PMMA system.

conversion of MMA during the different coating reactions. High conversions were observed in all cases, the polymerization rate being higher for the cases in which the seeds were prepared by micellar nucleation resulting in a large number of particles.

Changes in Particle Sizes During the Coating Stage

Figure 3 shows the evolution of the average size measured by DLS during the two stages (the formation of core seeds and the coating/formation of shell), for the different recipes of seeds. The results clearly show an increase in the average particle size, an indication of the shell formation on the seeds. The only exception was the reaction FP26 (Figure 3d), in which a small decrease in particle size during second stage is observed; this can probably be assigned, initially, to the large distribution of the

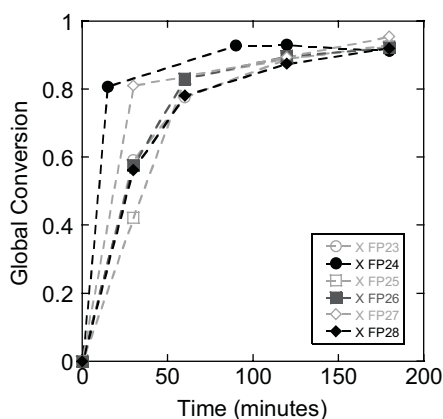
particles (PSD) as consequence nanoparticles with standard deviation broad as shown in Figure 4d, and secondly, a new (undesired) nucleation during the second stage. Anyway, the occurrence of some coalescence between the seeds and the new particles generated in the second stage is not discarded, being identified, in principle, by the rapid growth of the average size registered in DLS, where final average size was approximately double initial seed particles (observed in the Figures 3a and 3e). As result, there was a formation of core particles with discontinuous shell, as can be seen by the morphology of the final particles (micrographies shown later in Figure 6) where small particles produced by homogeneous nucleation (PMMA) are adhered to the larger particles.

The particle size distributions (histograms) also measured by DLS, for the seeds and for the particles at the end of the second stage are shown in Figure 4. Consistently with the results in Figure 3, the PSD of the particles after the second stage shifted towards the larger sizes after the coating with PMMA. In the case FP27 (Figure 4E), a generation of smaller particles in the second stage can be observed, an indication that nucleation of new particles during the coating stage occurred.

The number of particles per unit mass of emulsion (N_p) was estimated by the equation

$$N_p = \frac{M_0 X}{\rho_{pol} W_{tot} (\pi D_p^3 / 6)} \quad (1)$$

where M_0 is the initial weight of monomer, X is the overall monomer conversion, W_{tot}

**Figure 2.**

Conversion of MMA during the coating reactions (emulsion photopolymerizations).

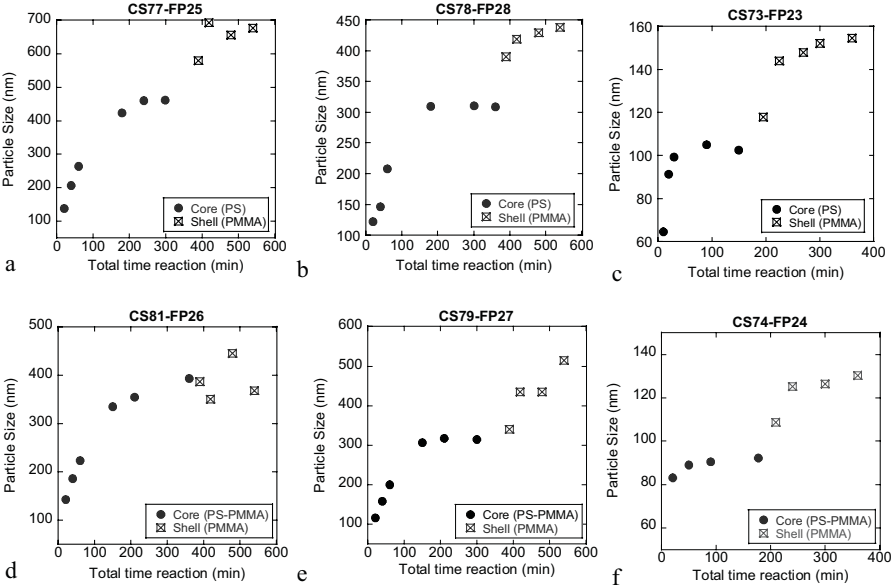


Figure 3. Changes in the average particle size during the first stage (production of core seeds of PS and PS-co-PMMA) and during the second stage (coating of particles, formation of PMMA shell).

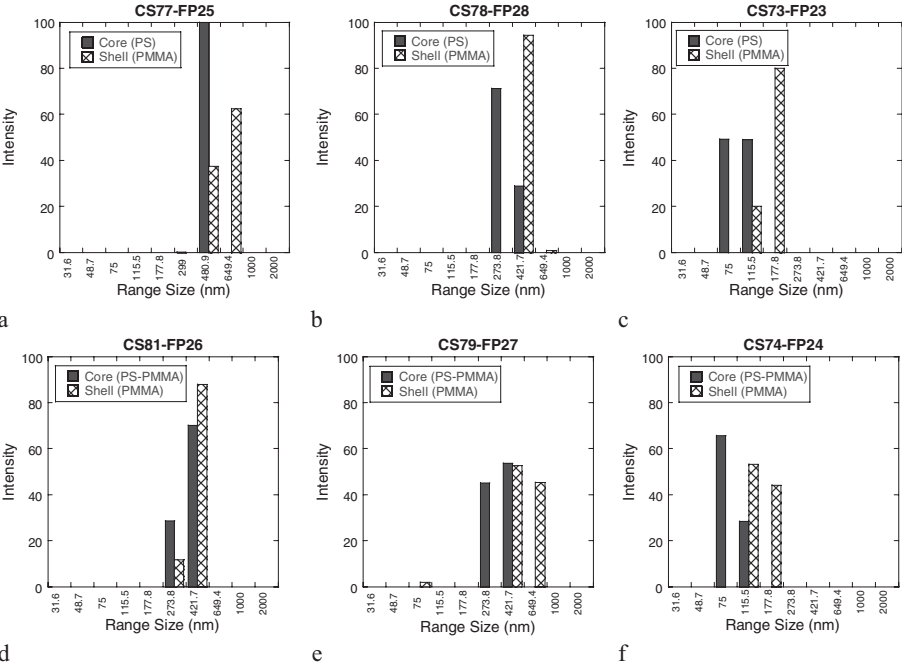


Figure 4. Histograms of the particle size distribution of the core seeds produced in the first stage and of the final particles after the second stage.

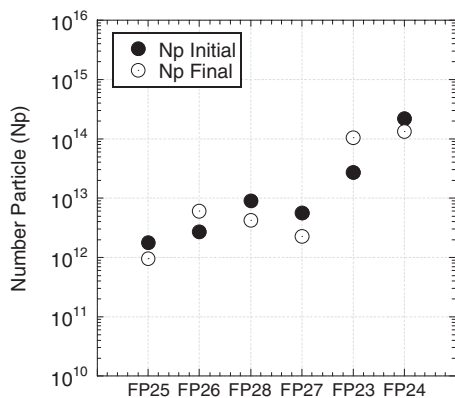


Figure 5. Number of particles (estimated by eq. 1) before and after the second stage of polymerization.

is the total weight of the emulsion, ρ_{pol} is the polymer density and D_p is the average diameter of the polymer particles. According to the results in Figure 5, there are small changes in N_p between the initial and after the coating process, which are almost within the uncertainty of the estimates using eq. (1). In principle, the increase in N_p can be attributed to the generation of new particles (nucleation), while the decrease in N_p can be due to the coalescence of the particles. In special, there may be cases of coalescence of particles nucleated during the second stage with seed particles, resulting in a different morphology (core-complete shell and core-discontinuous shell). Taking the case of runs FP27 and

FP25, respectively, this last morphology was confirmed by the authors in a previous work using atomic force microscopy (AFM), see Figure 6b.^[24]

TEM micrographs of the final latexes are presented in Figure 7. The final morphology of the particles exhibit two different phases, a dark core (as a result of the reaction between RuO₄ vapor and PS)^[25] and a lighter shell corresponding to the PMMA formed during the second stage of the process.

Note that Figure 7 also includes two additional TEM micrographs of mixtures of particles of homopolymer PS and homopolymer PMMA (Figure 7g and 7h), for facilitating the interpretation of the other micrographs. As can be seen, the coating of the seed particles has been successfully achieved for all cases. However, the coating was not uniform for all seeds, due to the differences in their surfaces that can facilitate or not the fixation of the shell over the core surface. It may be also seen that, for seeds produced without emulsifier and without crosslinker, some tendency to inversion or compatibility problems can occur due to a lack of anchoring agents to fix the shell polymer on to the core surface. Also, in case of not crosslinker used in the seeds, MMA monomer can diffuse within the core and create small PMMA submicrodomains (see Figure 7c).

When comparing the results of TEM and DLS, it is worth noting that there may be some differences between the average sizes

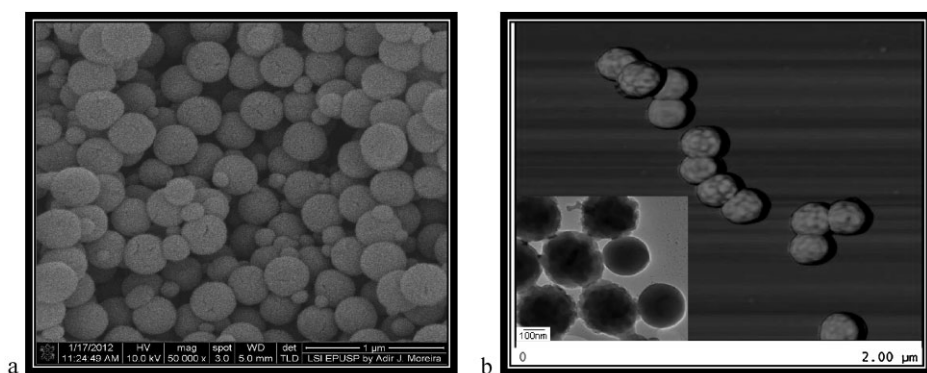


Figure 6. Morphology of the final particles FP27 (a) SEM and (b) AFM^[24]

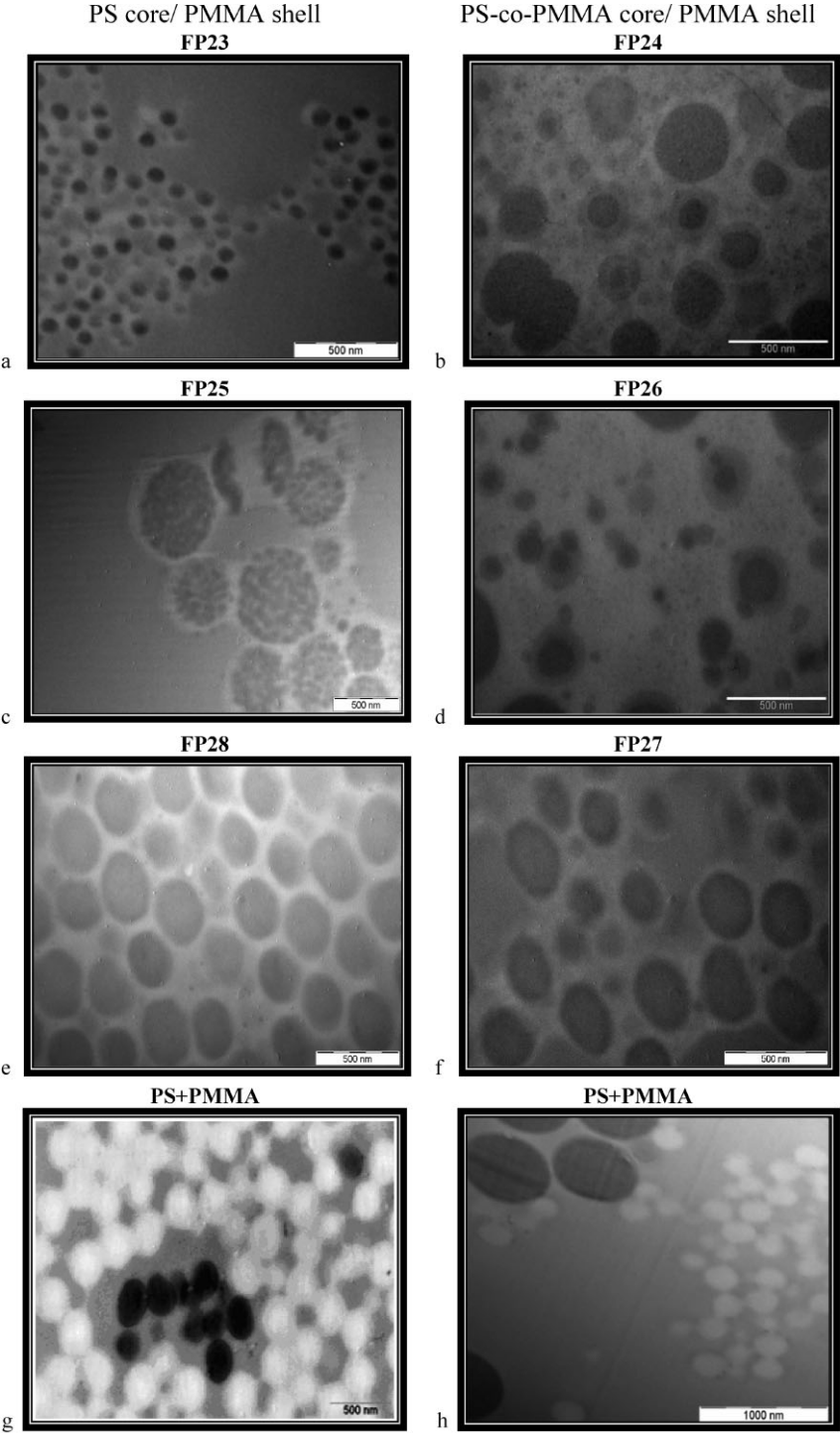


Figure 7. TEM images showing the morphology of the final particles obtained using different recipes (a-f) and of mixtures of particles of homopolymer PS and PMMA (g, h).

analyzed by DLS and observed by microscopy. These differences can be justified by the fact that, for broader particle size distribution (as the ones obtained in this work, see Table 3), one could expect larger average sizes for DLS when compared to TEM, because the DLS measures the size in intensity that is much higher for larger particles.

Thermal Analysis

An evaluation of the thermal transitions of each final latex was carried out and the glass transition temperature (T_g) of the prepared material was determined. In order to discriminate the thermal behavior of the core-shell structures in relation to separated phases, final latex of the seed particles of homopolymer PS and homopolymer PMMA were prepared with the same operational conditions (conventional, free-soap and SVBS/EDGMA ratio emulsion polymerization) and then mixed to simulate the incompatibility between the two polymer phases (the corresponding TEM images of these mixture of particles are presented in Figures Figure 7g and h). Moreover, the thermal analysis was performed for seeds of PS-co-PMMA to simulate the complete compatibility and the presence of a single phase. The Table 4 show the T_g values obtained and the

Table 4.

T_g values obtained by DSC.

	Values (°C)	
	T_g 1	T_g 2
Conventional emulsion polymerization		
PS + PMMA	101.5	125.4
FP23	105.3	124.3
FP24	110.5	123.8
PS-co-PMMA	110.4	
Free-soap emulsion polymerization		
PS + PMMA	106.5	134.5
FP25	108.5	130.2
FP26	109.7	130.5
PS-co-PMMA	104.8	
SVBS/EGMA ratio emulsion polymerization		
PS + PMMA	104.4	127.9
FP28	103.6	116.1
FP27	103.5	119.7
PS-co-PMMA	109.8	

Figures 8a, b and 8c show the DSC thermograms of the final latex by emulsion photopolymerization in comparison with the two previously mentioned references (particles of PS-co-PMMA and a mixture of PS and PMMA particles). The results show that the thermograms of the core-shell particles present two values of T_g , except that of sample FP25 which apparently present only a single T_g

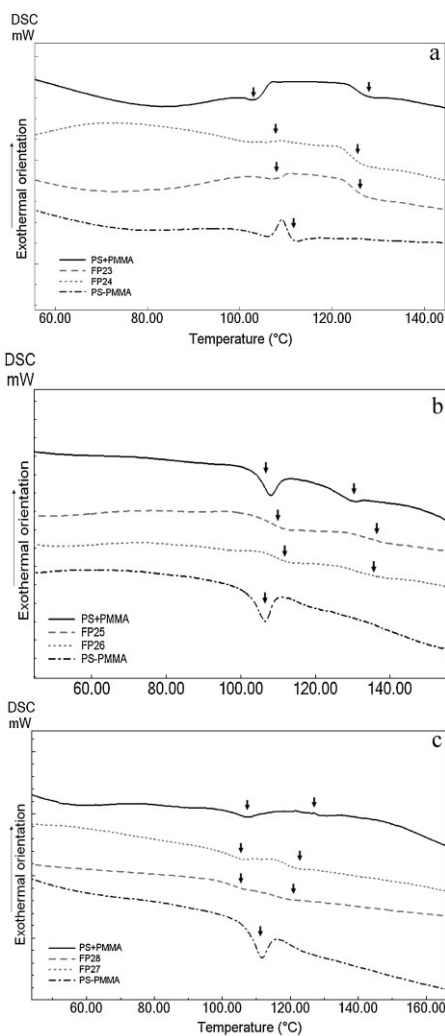


Figure 8.

DSC thermograms of the final latex particles obtained from (a) seeds prepared by conventional emulsion polymerization, (b) seeds prepared by emulsifier-free emulsion polymerization, and (c) seeds prepared using SVBS/EDGMA.

(Figure 8b), this can be attributed by microdomains of PMMA inserted into the PS, a behavior similar to that of a copolymer. Therefore, the thermograms of the core-shell particles point toward the presence of a partially miscible system with the presence of two phases (PS + PMMA or PS-co-PMMA + PMMA), differently of a miscible, single phase system such as the case of copolymer seeds (PS-co-PMMA).

Some shifts of the T_g values can be observed in the cases of higher content of shell PMMA, specially for the PS-co-PMMA seeds, and when particles of PMMA were nucleated during the second stage of the reaction.

Conclusion

The feasibility of the technique of emulsion photopolymerization for the preparation of nanostructured particles of the type of core(PS)-shell(PMMA) and core(PS-co-PMMA)-shell(PMMA) was demonstrated. According to the results by DLS and direct observation by TEM, in all cases the coating of the shells were observed, with better results for core seeds prepared using surface modifier and crosslinking agent. Also, the the DSC measurements indicated that the core-shell particles exhibit partially miscible behavior, which is different of that of presented by mixtures of homopolymer particles of the two polymers (i.e., PS particles and PMMA particles) and also of copolymer particles (particles of PS-co-PMMA).

Acknowledgements: The authors thank FAPESP – Fundação de Amparo à Pesquisa do Estado de São Paulo (Grant contract N° 2009/01581-1), CNPq – Conselho Nacional de Desenvolvimento Científico e Tecnológico and CAPESP for the financial support; BASF/Brasil for supplying monomers, Profa. Dra. S. Mendes and Mrs. S. Jared of the Laboratory of Cell Biology of Institute Butantan for the support with use of the TEM equipment, Profa. Dra. T. Bijovski of Institute of Biomedical Sciences ICB –USP for the help in the use of microtome, Mr. A. Moreira of Laboratory of Integrated

Systems (LSI-EPUSP) for the SEM micrographs, and Mr. H.J. Perez for the help during the experiments.

- [1] F. Carusso, *Adv. Mater.* **2001**, 13, 11.
- [2] Y. Mu, T. Qiu, X. Li, *Mater. Lett.* **2009**, 63, 1614.
- [3] R. H. Ottewill, A. B. Schotfield, J. A. Waters, N. S. J. Williams, *Colloid Polym. Sci.* **1997**, 275, 274.
- [4] H. T. Oyama, R. Sprycha, Y. XIE, R. E. Partch, E. J. Matijevic, *J. Colloid Interface Sci.*, **1993**, 160, 298.
- [5] L. Quaroni, G. Chumanov, *J. Am. Chem. Soc.*, **1999**, 121, 10642.
- [6] M. R. Rodriguez, M. G. Newmann, *Polímeros, Ciência e Tecnologia*, **2003**, 13, 276.
- [7] C. Villat, N. Pradelle-Plasse, B. Picard, P. Colon, *J. Mater. Sci. Eng.*, **2007**, 28, 971.
- [8] J. Stampfl, R. Infuhr, K. Stadlmann, N. Pucher, V. Schmidt, R. Liska, *Proceedings of the Fifth International WLT-Conference on Lasers in Manufacturing 2009*, Munich, June 2009.
- [9] A. C. Slongo, G. Pleti, M. C. F. Ramos, P. Campos, R. Vagner, P. K. T. Oldring, *Chemistry & Technology of UV&EB Formulations for Coatings, Inks & Paints: Vol 3 – SITA Technology – 1991*.
- [10] M. A. G. Bardi, L. D. B. Machado, *Radiat. Phys. Chem.*, **2011**, DOI: 10.1016/j.radphyschem.2011.11.068.
- [11] H.-J. Timpe, A. G. Rajendran, *Eur. Polym. J.*, **1991**, 27, 77.
- [12] K. Murata, A. Amamiya, T. Anazawa, *Macromol. Mater. Eng.*, **2003**, 288, 58.
- [13] H. Kihara, T. Miura, R. Kishi, *Polymer*, **2002**, 43(16), 4523.
- [14] S. E. Shim, Y. Shin, J. W. Jun, K. Lee, H. Jung, S. Choe, *Macromolecules*, **2003**, 36, 7994.
- [15] A. F. M. Silveiras, C. A. O. Nascimento, E. Oliveros, S. H. Bossmann, A. M. Braun, *Chem. Eng. Process.*, **2006**, 45, 1001.
- [16] X. Guo, A. Weiss, M. Ballauff, *Macromolecules*, **1999**, 32, 6043.
- [17] Y. Lu, A. Wittemann, M. Ballauff, M. Drechsler, *Macromol. Rapid Commun.*, **2006**, 27, 1137.
- [18] M. Schrinner, B. Haupt, A. Wittemann, *Chem. Eng. J.*, **2008**, 144, 138.
- [19] D. K. Balta, E. Bagdatli, N. Arsu, N. Ocal, Y. Yagci, *J. Photochem. Photobiol., A*, **2008**, 196, 33.
- [20] A. Kotera, K. Furusawa, Y. Takeda, Z. Z. Kolloid, *Polym*, **1970**, 239, 677.
- [21] G. W. Ceska, *J. Appl. Pol. Sci.*, **1974**, 18, 427.
- [22] A. M. Homola, M. Inoue, A. A. Robertson, *J. Appl. Pol. Sci.*, **1975**, 19, 3077.
- [23] W. Y. Chiu, C. C. Shih, *J. Appl. Pol. Sci.*, **1986**, 31, 2117.
- [24] M. V. Carranza, *Synthesis and characterization of core-shell nanoparticles of PS and PMMA obtained by emulsifier-free photoinitiated emulsion polymerization (in Portuguese)* **2011**, D. Sc. Thesis, Universidade de Sao Paulo, Brazil.
- [25] J. S. Trent, J. I. Scheinbeim, P. R. Couchman, *Macromolecules*, **1986**, 16, 589.